

Stability of FePt, FePt₃ Nanoclusters of Different Habits

D.G. Yakubik^{1*}, L.R. Sadykova², Yu.A. Zakharov², N.S. Zakharov², A.N. Popova², V.M. Pugachev¹

¹Kemerovo State University, 6 Krasnaya str., Kemerovo, Russia

²Institute of Coal Chemistry and Chemical Materials Science in the Federal Research Center of Coal and Coal Chemistry SB RAS, 18 Soviety sky Ave., Kemerovo, Russia

Article info

Received:

16 March 2022

Received in revised form:

30 April 2022

Accepted:

5 June 2022

Keywords:

Intermetallic
Solid solutions
Molecular dynamics
Nanoclusters
Diffraction-invisible phase

Abstract

Calculations of the total energy of Fe-Pt nanoclusters, corresponding in the phase diagram to the compositions of FePt, FePt₃ intermetallics and possessing either characteristic structures L1₀ and L1₂, respectively, or non-characteristic disordered structure A1, as well as various particle habits (cuboctahedra, icosahedra) are carried out by molecular dynamics for the first time. The dependences of cluster stability on their size and temperature are plotted, along with the schemes of temperature transformations of cluster morphology and the dependence of the melting points of the clusters with these structures and habits on their size. The size range (2–8 nm) corresponds to the sizes of particles observed by high-resolution electron microscopy. It is shown that the species play an essential part in the phase transformations proceeding under heating in the nanostructured system Fe-Pt and leading to the formation of nanocrystals with highly ordered L1₀ structure possessing giant coercivity are cubic nanoclusters with the ordered structures L1₀ and L1₂. With an increase in cluster size, their stability and melting points increase, tending to saturation of the dependencies within the size range above 10 nm. The least stable clusters are those of intermetallics with non-characteristic disordered structure A1 and icosahedral habit.

1. Introduction

One of the hot spots of materials science in nano-sized polymetallic systems is the problem of obtaining FePt particles of equiatomic composition as blockless nanocrystals (NC) with tetragonal structure L1₀ at high ordering [1–6]. The most practical synthesis method is the joint reduction of the components (Pt, Fe) from the mixtures of the aqueous solutions of precursors [1, 6]. In practical respect, the relevance of solving this problem is due to the fact that, because of the features of atomic structure [1–4], this system possesses a unique combination of properties for nanopolymetals: giant coercivity (estimated as up to 9 T) [4–6] and rather high saturation magnetization and Curie temperature, high magneto-optical anisotropy, etc., which determines the high potential of this system for micro-(nano)electronics, micro-(nano)magnet-

ic engineering, in developing the media with the high density of magnetic information record [7–10]. Meeting the above-listed requirements, FePt NC are probable candidates for the development of memory elements with maximal record density, given the possibility to obtain these elements with a size of about 5 nm, with the conservation of ferromagnetic state up to a temperature of 300–320 K, possessing a high temperature of the transition into the super-paramagnetic state because of the giant coercivity.

Despite the relevance of this problem and enormous effort aimed at solving it, it has not been solved yet, as reported in [11–12], because of unusual phase compositions of the nanostructured Fe-Pt system obtained through Red-Ox reactions and the complicated nature of phase transformations during the transition of nanoclusters under heating from the initial non-equilibrium state of the target phase of highly ordered intermetallic (IM) with L1₀ structure (Fig. 1).

*Corresponding author.

E-mail addresses: den@kemsu.ru

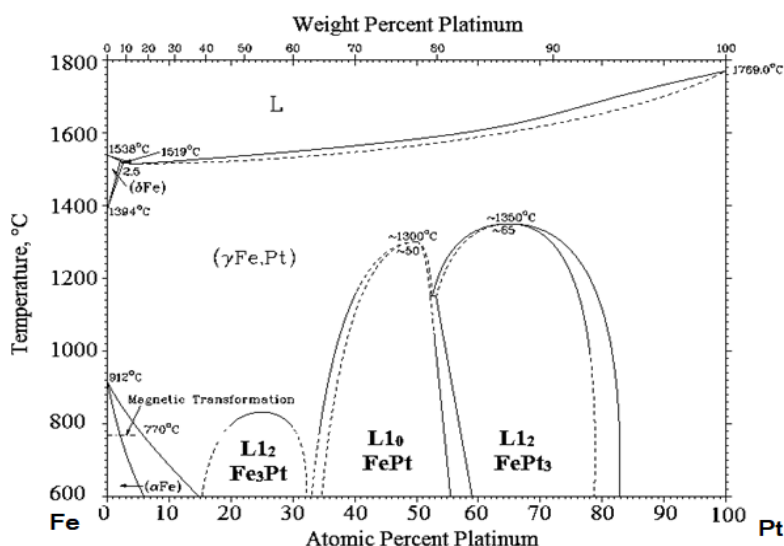


Fig. 1. Phase diagram of FePt [13].

The specificity of phase transformations resulting in the formation of the target phase L1₀ is in their occurrence as a sequential series of reactions of solid-solid type, with the formation of nano-phases in the sequence A1→L1₂(IM FePt₃)→L1₀ (IM FePt), while one reagent is the nanoparticles of FePt₃, FePt, possibly Fe₃Pt phases that cannot be detected by diffraction [11]. Their essential role in phase transformations leading to the formation of the target L1₀ phase, along with the practical impossibility of studying their morphology and atomic structure experimentally, makes calculations the major tool of their investigation.

Along with the above considerations, a relevant task is a calculation of the stability of the formed IM FePt particles with L1₀ structure in the above-show size range (4–6 nm) and their properties (habit of the particles, melting point, and ordering degree).

In the present work, we describe the results of calculations of nanoclusters (NC) with the structures of disordered *fcc* solid solution (A1 type), ordered *fcc* FePt₃ IM (L1₂ type), and ordered tetragonal FePt IM (type L1₀), i.e. the forms in which the particles of diffraction-invisible phases (DIF) may be formed, in all the cases of cuboctahedral (corresponding to macro objects) and icosahedral (more favorable for nanosamples because of the minimal surface energy) habits, within the size range 3 to 8 nm, which is relevant according to the experimental data (see below). For the first time in the FePt nanosystem, the calculations have been carried out by molecular dynamics, as the most precise method, which is convenient for the calculation of multi-component metal systems.

2. Experimental

2.1. Object preparation

Nanostructured FePt powders (NSP) were obtained in the reactor thermostated at 80 °C by the co-reduction of the metals with hydrazine (as hydrazine hydrate, taken in 10-fold excess over the stoichiometric amount) from the mixtures of aqueous solutions (0.1 mol/L) of HPtCl₆ 6H₂O, FeSO₄ 7H₂O, CoSO₄ 7H₂O (all reagents were of analytically pure grade). Synthesis conditions and details were described in [12, 14].

2.2. Experimental investigation methods

The structure, phase compositions and details of phase structures of NSP were studied by X-ray diffraction using the Bruker D8 ADVANCE A25 diffractometer (Germany), with Cu K α radiation, at $\lambda = 1.5406 \text{ \AA}$, with Ni filter at the secondary beam. Measurements were carried out within the 2 angle range of 200–1400, with a scan step of 0.020. Data collection and XRD processing were carried out using the Diffrac.Suite.Eva (V3.1) software package.

The composition of diffraction-visible phase was determined with the help of ICDD PDF-2 database and the empirical dependence between the composition and average volume per one atom in the unit cell [11]. Electron microscopic observation was carried out with a JEOL JEM 2100 microscope (JEOL Ltd, Japan) in the light field mode. The sample preparation for highly magnetic NSP was described in [15].

2.3. Theoretical analysis

Calculation of the total energy of the clusters was carried out with the help of LAMMPS software [16] by molecular dynamics, using the MEAM-2NN potential [17]. The parameters of the potential were taken from [18]. The simulation was carried out within the framework of a micro-canonical (NVT) ensemble using the Nosé-Hoover thermostat. The thermostat constant and the time step were determined in preliminary calculations to be 0.012 and 0.001 ps, respectively.

Atomic coordinates were determined in the WinPython software [19] using the ASE library [20]. The initial form of nanoclusters includes regular cuboctahedra and icosahedra with atomic positions and interatomic distances characteristic of the bulk samples of corresponding phases.

Visual images of cluster transformations and

their atomic structures were obtained in the Ovito software [21].

3. Results and discussion

The XRD analysis of Fe-Pt samples containing Fe within the range of 7–24 at.% detects the only phase, with reflections corresponding to the fcc lattice (type A1) as shown in Fig. 2a. The compositions of this phase, calculated according to the procedure described in [11], are presented in Fig. 2b. According to these results, according to the phase diagram of the Fe-Pt system (Fig. 1), the detected phase is a Pt-rich solid solution (SS) with the upper limit of Fe solubility in Pt 11.4 ± 0.7 at.%. It follows from this that the Fe-Pt samples with Fe content above the limit of their solubility in Pt contain, along with the SS phase detected by XRD, also a diffraction-invisible, Fe-rich phase

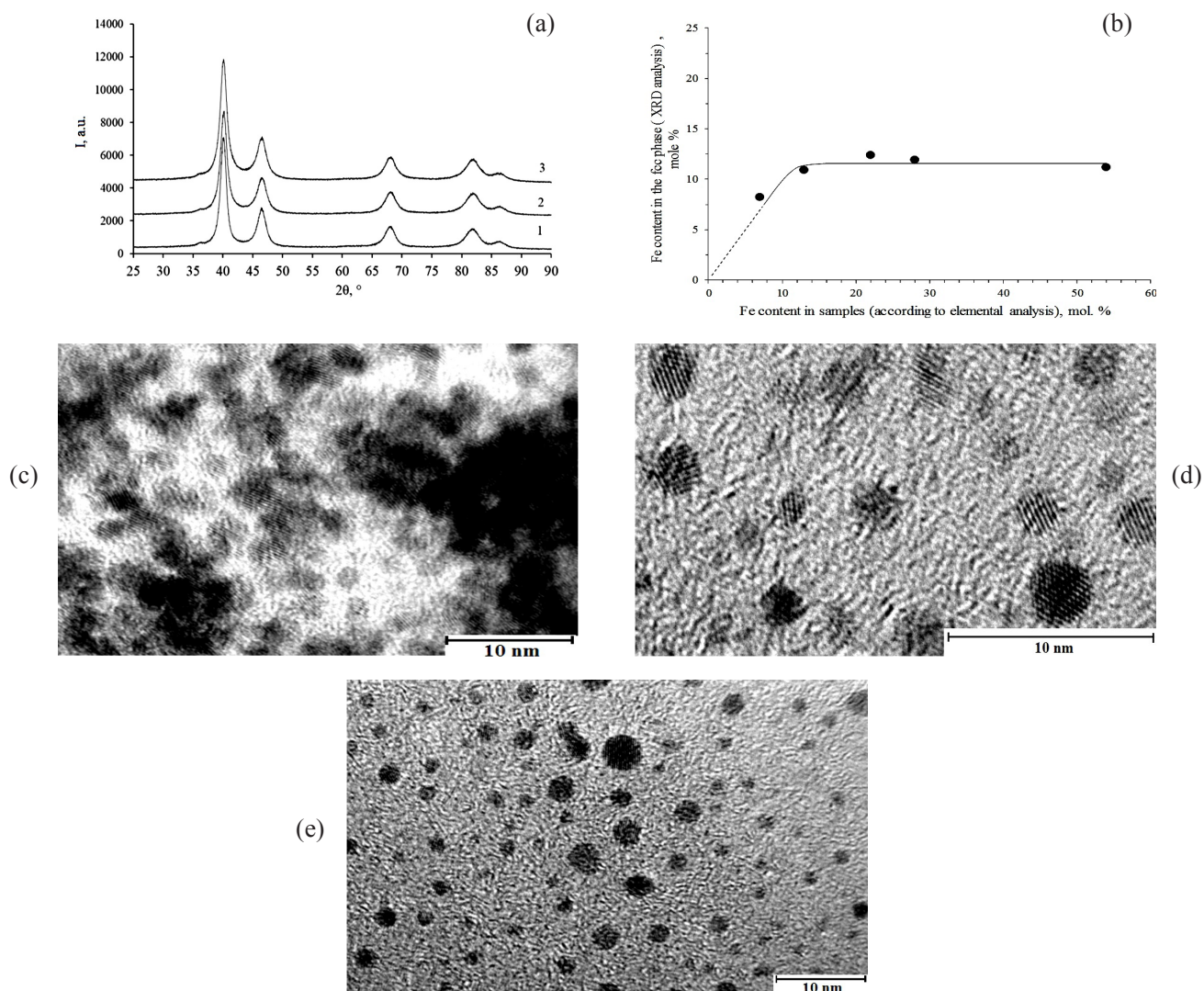


Fig. 2. (a) – X-ray diffraction patterns of the samples of FePt nanoparticles with 7 (1), 19 (2) and 24 (3)% Fe; (b) – dependence of the composition of the *fcc* phase (according to XRD data) on sample composition; (c–e) – typical TEM microphotographs of FePt particles..

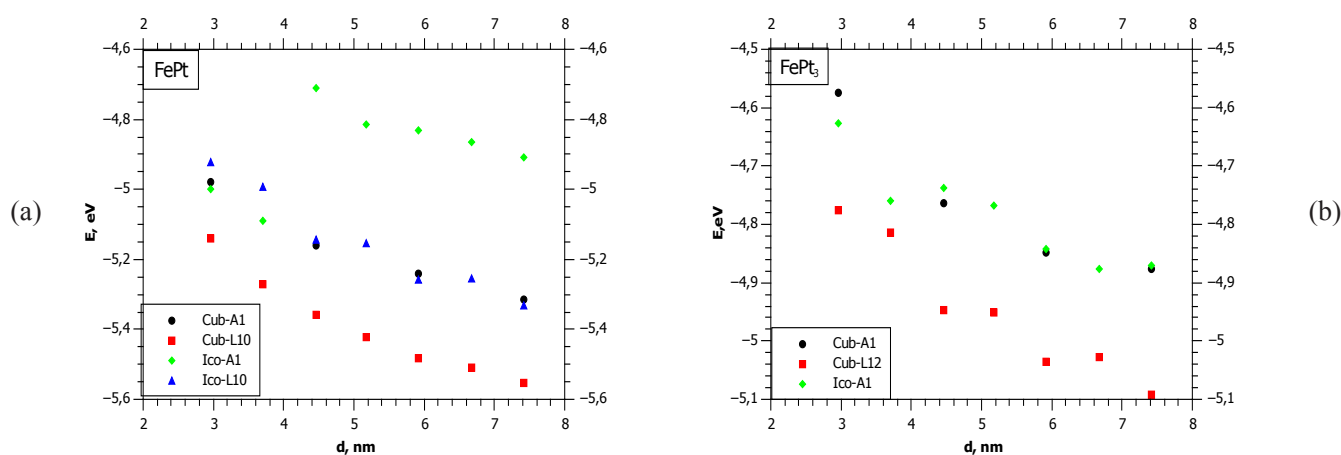


Fig. 3. Size dependence of the energy of FePt (a) and FePt₃ (b) nanoclusters with different structures and habits.

(or phases). Its diffraction invisibility is connected with ultra-small particle size and consequent substantial broadening of diffraction peaks, which hinders their observation against the background of reflections from the *fcc* phase (A1), close in composition, with lower scattering efficiency because of lower Pt content, and with the possibility of the amorphous structure of nanoclusters.

In the TEM images one can see, along with abundant *fcc* SS nanocrystals, the particles with a size of 2–4 nm, often adjacent to the surface of the former particles (Fig. 2 c), as well as smaller formations (Fig. 2 d).

The size dependences of the total energy of the nanoclusters of different habits, with e atomic ratios corresponding to IM composition FePt, FePt₃, at 0 K are shown in Fig. 3. One can see that the most stable NC are those of the ordered phases L1₀ and L1₂ (IM FePt, FePt₃, respectively), shaped as cuboctahedra, which is characteristic of them in the bulk state. The results obtained by HRTEM correspond to these observations. Some HRTEM images of nanoparticles 3–4 nm in size exhibit atomic rows with the distance between them corresponding to the 111 plane of the *fcc* lattice (Fig. 2e).

The least stable NC are those with the icosahedral habit with disordered A1 structures, which are not characteristic of IM. Amorphization of NC causes a decrease in stability for each of the structures under consideration. The most stable NC of FePt IM are those shaped as cuboctahedra.

An increase in cluster stability with an increase in their size is observed, as established experimentally and by simulation.

The calculated dependences of the total energy of nanoclusters on temperature for NC with different structures and habits are shown in Fig. 4.

Transformations of NC morphology for three different shapes (the major ones under consideration) are presented in Fig. 5.

The sequences of stability change with an increase in NC size under variation of cluster habit and structure qualitatively correspond to those shown in Fig. 3. With an increase in temperature, cluster stability decreases because of gradual disordering shown in Fig. 5.

These data were used to evaluate the dependences of melting points of FePt and FePt₃ IM cubic clusters, which are most stable according to calculation results and correspond to the phase diagram, and the dependencies are presented in Fig. 6. The shape of $T_m = f(D_{nm})$ curve is typical for these dependencies, obtained experimentally and theoretically for many nanosized metal systems. In our case, the curve tends to be saturated near sizes larger than 8 nm. Melting points are higher for more stable (Fig. 3) cubic IM FePt clusters with L1₀ structure; with an increase in NC size from 3 to 7.5 nm, the difference between melting points decreases, which is in inverse relation to the change of NC stability within this size range and requires additional consideration.

According to the phase diagram (Fig. 1), NC corresponding to FePt and FePt₃ IM melt after transformation into A1 structure. Calculations show (Fig. 3) that the stability of the clusters with equiatomic composition with A1 structure is higher than the stability of FePt₃ NC with the same structure and the same size. So, the difference in the melting points of bulk samples of the corresponding compositions (Fig. 1) from their NC (Fig. 6) is larger within the whole size range of the crystallites of FePt₃ composition.

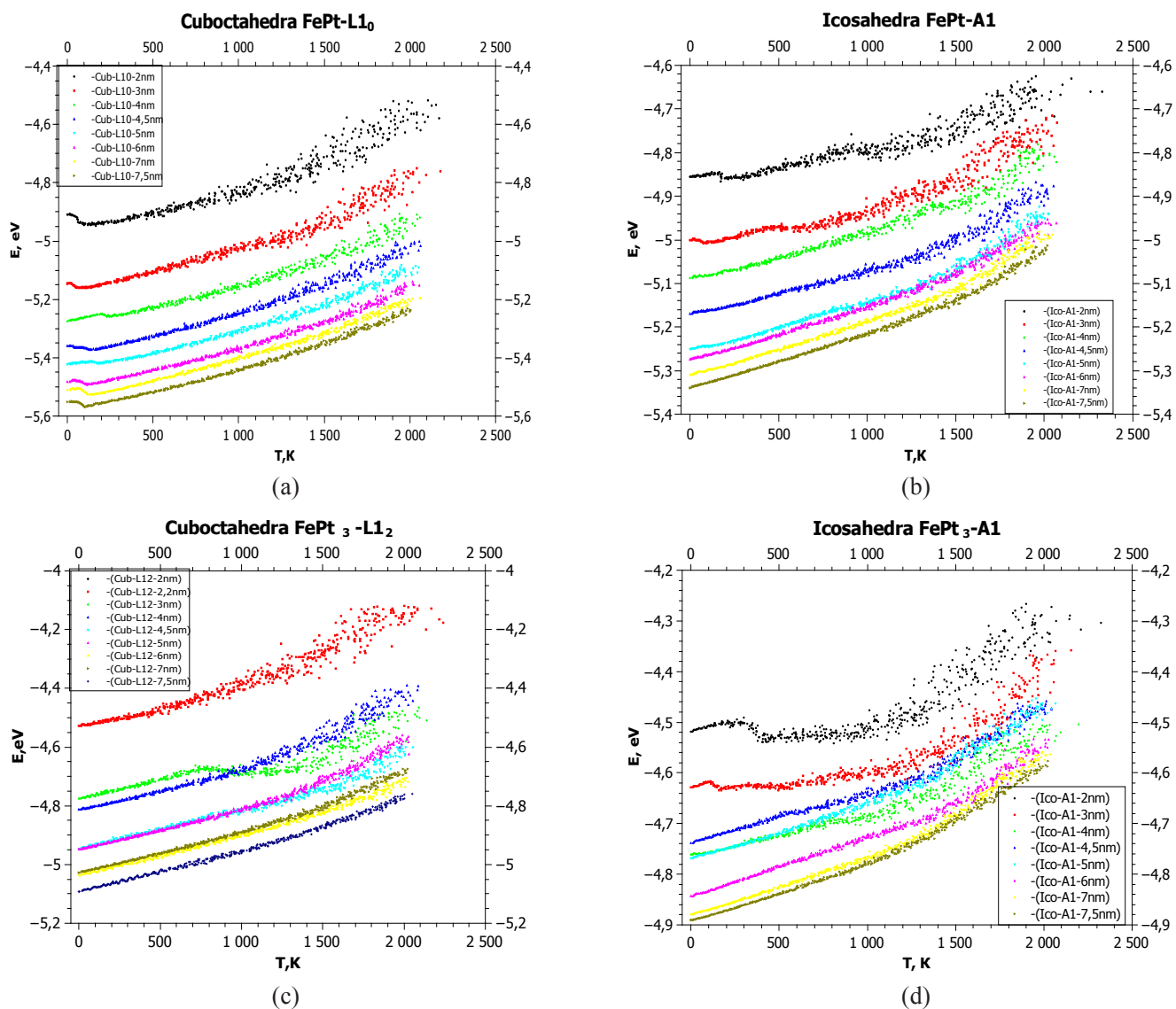


Fig. 4. Temperature dependences of the energy of nanoclusters of different size: cubic FePt with L1₀ structure (a), icosahedral FePt with A1 structure (b), cubic FePt₃ with L1₂ structure (c), icosahedral FePt₃ with A1 structure (d).

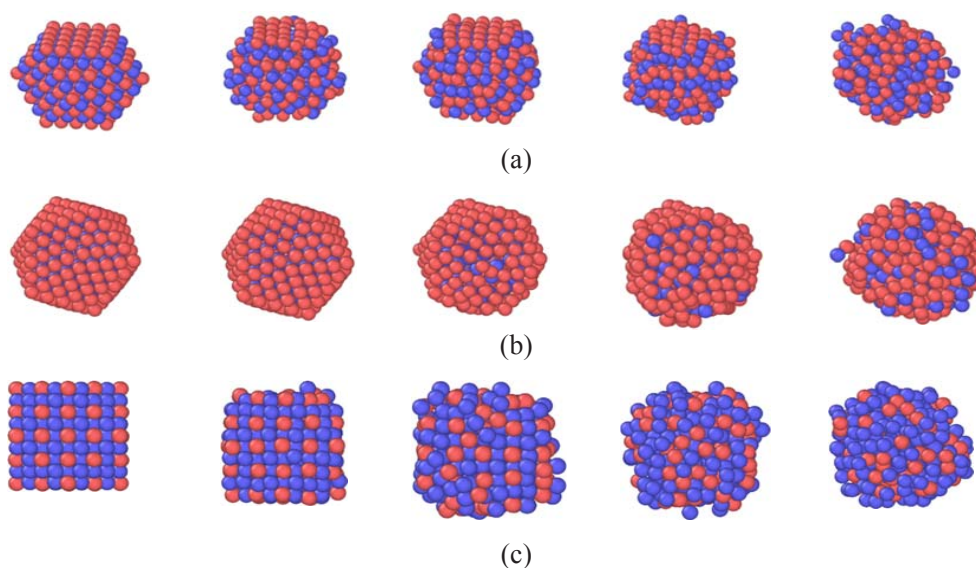


Fig. 5. Stability of the nanoclusters of different sizes under heating: (a) – cuboctahedron, L1₀ structure; (b) – icosahedron; (c) – cuboctahedron FePt₃, L1₂ structure.

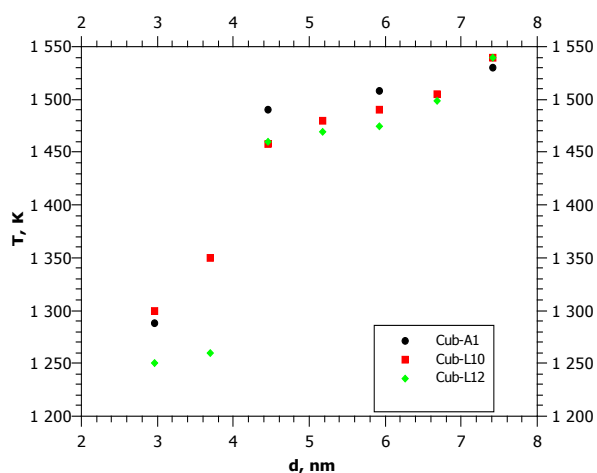


Fig. 6. Melting points of FePt, FePt₃ nanoclusters.

4. Conclusion

Results described show that the particles smaller than 2–3 nm, undetectable by X-ray diffraction but observable by HR TEM, and play an essential part in the phase transformations of nanostructured FePt particles under heating with the formation of particles in the highly ordered L1₀ structure with unique magnetic properties, are the ordered clusters of cubic shape with L1₂ and L1₀ structures corresponding to the phase diagram of FePt.

Acknowledgment

The work was carried out using the equipment of the Shared Equipment Center at the FRC CCC SB RAS within the State Assignment for the FRC CCC SB RAS for 2021–2023 (Project No. 121031500211-9).

References

- [1]. L. Yang, Y. Jiang, N. Kadasala, X. Zhang, C. Mao, Y. Wang, H. Liu, Y. Liu, Y. Yan, *J. Solid State Chem.* 22 (2014) 167–170. DOI: 10.1016/j.jssc.2014.03.041
- [2]. G. Kovacs, S.M. Kozlov, I. Matolinova, M. Vorokhta, V. Matolin, K.M. Neyman, *Phys. Chem. Chem. Phys.* 17 (2015) 28286–28297. DOI: 10.1039/C5CP01070E
- [3]. S. Schneider, D. Pohl, S. Löffler, J. Rusz, D. Kasinathan, P. Schattschneider, L. Schultz, B. Rellinghaus, *Ultramicroscopy* 171 (2016) 186–194. DOI: 10.1016/j.ultramicro.2016.09.009
- [4]. T.G. Klemmer, N. Shukla, C. Liu, X.W. Wu, E.B. Svedberg, O. Mryasov, R.W. Chantrell, D. Weller, *Appl. Phys. Lett.* 81 (2002) 2220–2222. DOI: 10.1063/1.1507837

- [5]. J. He, B. Bian, Q. Zheng, J. Du, W. Xia, J. Zhang, A. Yan, J. Ping Liu, *Green Chem.* 18 (2019) 417–422. DOI: 10.1039/C5GC01253H
- [6]. S.B. Dalavi, R.N. Panda, *J. Magn. Magn. Mater.* 428 (2017) 306–312. DOI: 10.1016/j.jmmm.2016.12.105
- [7]. Y. Liu, K. Yang, L. Cheng, J. Zhu, X. Ma, H. Xu, Y. Li, L. Guo, Z. Liu, *Nanomed. Nanotechnol.* 9 (2013) 1077–1088. DOI: 10.1016/j.nano.2013.02.010
- [8]. Y. Shi, M. Lin, S. Liang, *J. Nanomater.* (2015) 467873. DOI: 10.1155/2015/467873
- [9]. C.L. Dennis, R. Lvkov, *Int. J. Hyperth.* 29 (2013) 715–729. DOI: 10.3109/02656736.2013.836758
- [10]. X. Sun, Y. Huang, D. Nikles, *Int. J. Nanotechnol.* 1 (2004) 328. DOI: 10.1504/IJNT.2004.004914
- [11]. V.M. Pugachev, Y.A. Zakharov, A.N. Popova, D.M. Russakov, N.S. Zakharov, *J. Phys. Conf. Ser.* 1749 (2021) 012036. DOI: 10.1088/1742-6596/1749/1/012036
- [12]. N.S. Zakharov, V.M. Pugachev, Yu.A. Zakharov A.N. Popova, *Chem. Sust. Dev.* 29 (2021) 536–542. DOI: 10.15372/CSD2021331
- [13]. Binary Alloy Phase Diagrams—Second edition. T.B. Massalski, Editor-in-Chief; H. Okamoto, P.R. Subramanian, L. Kacprzak, Editors. ASM International, Materials Park, Ohio, USA. December 1990. xxii, 3589 pp., 3 vol. DOI: 10.1002/adma.19910031215
- [14]. N.S. Zakharov, A.N. Popova, Yu.A. Zakharov, V.P. Pugachev, *J. Phys.: Conf. Ser.* 1749 (2021) 012012. DOI: 10.1088/1742-6596/1749/1/012012
- [15]. N.S. Zakharov, A.N. Popova, Yu.A. Zakharov, D.M. Russakov, *J. Phys.: Conf. Ser.* 1749 (2021) 012011. DOI: 10.1088/1742-6596/1749/1/012011
- [16]. Software official website: <https://www.lammps.org> Visit date: 16.05.2022
- [17]. B.J. Lee, M.I. Baskes, H. Kim, Y.K. Cho, *Phys. Rev. B* 64 (2001) 184102. DOI: 10.1103/PhysRevB.64.184102
- [18]. J. Kim, Y. Koo, B.-J. Lee, *J. Mater. Res.* 21 (2006) 199–208. DOI: 10.1557/jmr.2006.0008
- [19]. Software official website: <https://winpython.github.io> Visit date: 16.05.2022
- [20]. A.H. Larsen, J.J. Mortensen, J. Blomqvist, I.E. Castelli, et al., *J. Condens. Matter Phys.* 29 (2017) 273002. DOI: 10.1088/1361-648X/aa680e
- [21]. A. Stukowski, *Modelling Simul. Mater. Sci. Eng.* 18 (2010) 015012. DOI: 10.1088/0965-0393/18/1/015012